

Calculations of Rocket Plume Afterburning Coupled to Reacting Base Recirculation Regions

Andrew C. Victor*

Naval Weapons Center, China Lake, Calif.

Afterburning of combustible plume species with air is the most striking effect noted in observations of low-flying missiles (less than 30-km alt). Because afterburning raises the temperature of the plume, it intensifies the physical and chemical processes that cause plume signature effects. In systems with relatively cool exhausts, the onset of afterburning is delayed until the missile speed exceeds some minimum value (about Mach 2.2). The onset of afterburning in these cases has been attributed to the effect of combustion in a recirculation zone at the base of the missile. A model of equilibrium combustion in the base region was coupled to a chemical kinetic model of downstream plume mixing and afterburning in order to perform the calculations for this study. The calculations made with the combined model confirm observations of plumes which afterburn only after the base region has ignited. The calculations also indicate that the rocket motor mass flow rate has an important influence on plume afterburning. It also is calculated that, for systems with hot exhausts, the base has no important effect on afterburning in the rest of the plume.

Nomenclature

C	= ratio of mass of jet gas to total gas at x, r
\dot{m}	= mass flow rate
r	= radial distance from plume centerline
t	= residence time of gas in base region
u_e	= velocity of external flow in base region
u_j	= velocity of jet flow in base region
x	= longitudinal distance
ϵ	= area ratio of nozzle exit to nozzle throat
ρ	= gas density at x, r

Subscripts

B	= base region
e	= external
i	= internal
s	= limiting streamline or startline for aft-plume calculation

Introduction

ALTHOUGH the improved computed models¹⁻⁸ that have been developed in the past few years for calculating the flowfields of low-altitude (less than 30 km) rocket exhaust plumes have been quite successful in a number of cases, they fail in those instances for which the combustion occurring in the vicinity of the missile base must be considered as a flameholder for ignition of afterburning downstream in the plume. Figure 1 illustrates the power of base recirculation to act as a flameholder for afterburning. The figure shows two successive frames of 16-mm motion picture film taken at a frame rate of 24 sec⁻¹. The subject was a small rocket motor of about 220-N thrust with a 12.7-cm-diam base in a wind tunnel with a freestream air speed of 850 m-sec⁻¹ at a simulated altitude of 11.5 km. The freestream flow was accelerating during the motor firing, and the lower exposure in the figure corresponds to a freestream velocity about 5 m/sec higher than does the upper exposure. The afterburning continued at the higher level throughout the remainder of the motor firing. The photographs indicate that only a very slight difference in freestream velocity separates the conditions for ignition and nonignition in the base recirculation region. We

also have observed that the tendency for combustion to attach to the base, as in the lower image of Fig. 1, increases as the nozzle exhaust velocity decreases. This has been observed many times as rocket motor firings in wind-tunnel tests "tail off" toward the end of burn. The tendency for burning to occur in the base region is reduced as the ratio of the base diameter to the nozzle exit diameter is reduced and can be eliminated in some cases by a boattail shape tapering to the missile base.

Sophisticated computational methods have been described for simultaneously solving the elliptical partial differential equations of the flow dynamics and chemical kinetics in the base recirculation zone⁹ and for coupling the results to mixing and afterburning plumes.¹⁰ The present study involved coupling a much simpler base combustion model with equilibrium chemistry¹¹ to a parallel flow plume model incorporating chemical kinetics.² Since the plume model used assumes constant pressure in the plume, the effects of plume shock structure were not included in the analysis.

Base Recirculation Model

The base recirculation model used in this study was developed by Smoot et al. at Brigham Young University (BYU)¹¹ on the basis of the work of Beheim et al.^{12,13} The model, shown schematically in Fig. 2, accounts for chemical effects with the assumption that all chemical reactions go to equilibrium in the base recirculation region. In order to see if this is a reasonable assumption, calculations were made to compare equilibrium species concentrations with the results of chemical calculations made using a single streamline kinetics program¹⁴ applied to the base region as if it were a perfectly stirred reactor.¹⁵

In order to apply this "stirred reactor" model, it is necessary to determine the input or output mass flow rate and the volume of the base region and hence the residence time of gas in the region. The mass of gas in the base region is determined easily from geometry and gas density values calculated by the BYU program. Although mass flow rate of gas leaving the base region is not given by the BYU program, it can be determined by assuming that it comprises all of the base gas passing through the trailing shock (i.e., external to the limiting streamlines). Then, for the internal flow,

$$\dot{m}_{B_i} = \frac{2\pi u_i}{(1-C_B)} \int_{r_{s,i}}^0 (1-C) \rho (C-C_B) r dr \quad (1)$$

Received March 9, 1977; revision received June 3, 1977.

Index category: Jets, Wakes, and Viscid-Inviscid Flow Interactions.

*Physicist, Propulsion Development Department, Associate Fellow AIAA.

Fig. 1 Transition of rocket exhaust base region combustion and aft-plume ignition shown in two successive frames of motion picture film at 24 frames/sec. Freestream velocity was 850 m/sec in upper frame and 855 m/sec in lower at simulated altitude of 11.5 km.



and for external flow,

$$\dot{m}_{B_e} = \frac{2\pi u_e}{C_B} \int_{r_{s,e}}^{\infty} C\rho(C_B - C)rdr \quad (2)$$

and for the total flow,

$$\dot{m}_B = \dot{m}_{B_i} + \dot{m}_{B_e}$$

The residence time of gas in the base (t) then is obtained by dividing base region mass by the mass flow rate:

$$t = (\pi/2) (r_e^2 - r_i^2) x_B \rho_B / \dot{m}_B$$

where $x_B = x_S - x_0$. This is essentially the same problem as a gas moving a distance x_B at a velocity $u = x_B/t$. For the case examined (case of Fig. 7), $x_B = 0.15$ m, $u = 70$ m/sec, and $t = 0.002$ sec. It was assumed that the starting composition at x_0 was the appropriate mixture of jet effluent and air ($C_4 = 1$, $C_3 = 0$) to give the base composition ($C_7 \sim 0.5$) after combustion to equilibrium. The results in Table 1 show that the approach to equilibrium is substantial in the base region, and thus the assumption of chemical equilibrium gives a good approximation even for the free radial species concentrations. The assumption of chemical equilibrium in the base region becomes progressively worse as the dimensions of the region decrease or as the pressure in the base region decreases.

Aft-Plume Model

The Low Altitude Plume Program (LAPP) developed by the AeroChem Research Laboratories² was used for the aft-plume calculations. Several modifications were incorporated:

1) The Stowell-Smoot correlation for the turbulent mixing coefficient¹¹:

$$K = 0.0467(M_{0.5})^{0.0574}(\rho_1/\rho_5)^{-0.7094} \times [(u_6 + u_5)/(u_6 - u_5)]^{0.742}$$

2) A modified aft-plume longitudinal pressure variation¹:

$$P = P_{\infty} \{1 + [(P_i/P_{\infty}) - 1]e^{-bx}\} \quad (3)$$

where P_i is the pressure behind the trailing shock and P_{∞} is ambient pressure. Determination of appropriate values of P_i and b has been described elsewhere.

In other respects, the use of the LAPP code is as described in the literature² for inhomogeneous starting conditions. The user must define the number of stream tubes at the start of the aft-plume calculation and the temperature, velocity, and

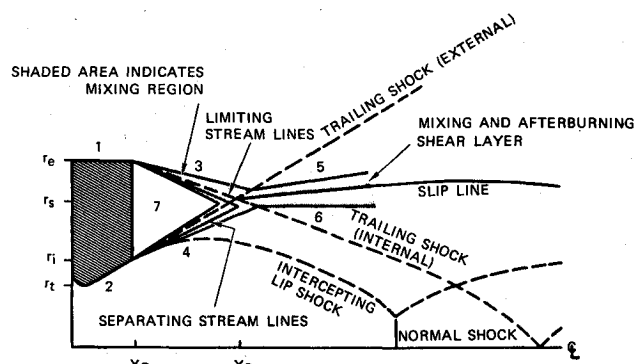


Fig. 2 Schematic drawing of plume including base effects. Regions shown: 1) external freestream flow, 2) internal nozzle flow, 3) external base region flow, 4) internal base region flow, 5) external exhaust plume flow, 6) internal exhaust plume flow, and 7) base recirculation zone.

species concentrations in each stream tube. The exhaust jet was assumed to be homogeneous except for the stream tube or tubes, which contain the effluent from the base region.

Coupling of Base Model to Aft-Plume Model

For tactical low-altitude missile propellant performance and plume calculations, one normally may assume uniform conditions (temperature, pressure, species concentrations) across the nozzle exit plane (the starting point for aft-plume turbulent mixing with air). In order to couple the effect of base mixing with the aft-plume, it is convenient to assume that turbulent mixing starts downstream of the base region. Therefore, the selected starting position for the aft-plume calculation is at the trailing shock (x_S in Fig. 2). The plume is no longer uniform at the start of turbulent aft-plume mixing but instead is composed of a central core surrounded by internal and external free shear layers. These shear layers are separated from each other by the slip line. If we assume that the flow properties at the slip line correspond to those at the limiting streamlines upstream of the trailing shock, then external and internal velocities at the slip line are given, respectively, by

$$u_e = u_5 (C_B - C_{s,e}) / C_B \quad (4)$$

$$u_i = u_6 (C_{s,i} - C_B) / (1 - C_B) \quad (5)$$

where the subscripts 5 and 6 correspond to regions defined in Fig. 2. This situation is considerably different from a typical

Table 1 Comparisons of equilibrium and nonequilibrium chemistry in the base region (propellant C)

Species	Ratio of species concentrations	
	Start ^a equilibrium	Kinetic ^b equilibrium
N ₂	0.93	0.97
O ₂	6.07	1.60
CO ₂	0.7	0.83
H ₂ O	0.39	0.90
HCL	1.24	0.82
CO	1.65	1.40
H ₂	7.95	1.50
CL	2.5 (-9) ^c	1.40
OH	8.0 (-12)	1.54
H	1.3 (-8)	2.59
O	7.4 (-11)	2.64

^a Unreacted mixture of jet effluent and air.

^b After reacting for 0.002 sec; species were substantially at equilibrium in 0.01 sec.

^c Parenthesized numbers are exponents of 10 [e.g., 2.5 (-9) = 2.5 × 10⁻⁹].

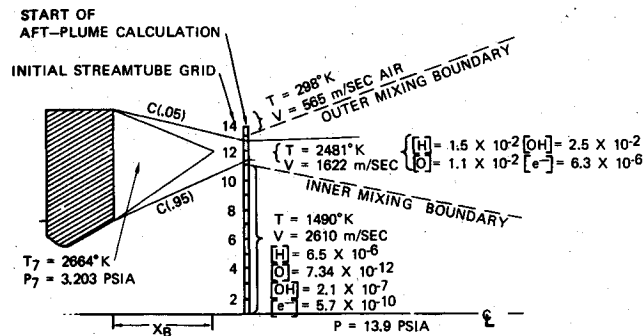


Fig. 3 Simplified schematic of missile plume for coupling base region to constant-pressure aft-plume model.

freejet boundary layer [Eq. (6)], for which the velocity varies continuously across the layer:

$$u = C(u_6 - u_5) + u_5 \quad (6)$$

Although the base recirculation region is important in itself through its influence on missile aerodynamics, heating of the missile base, and as a local source of free electrons and radiation, it also has a great potential to influence the aft-plume by modification of plume properties at the starting point of the aft-plume. The major factors causing modifications to the aft-plume are

1) increased temperature in the shear layer at the start of mixing, 2) increased concentration of free radicals in the shear layer at the start of mixing, and 3) modified radial and longitudinal pressure distribution in the aft-plume because of the effect of the base region on core flow and of the trailing shock.

The first two modifications are incorporated easily into low-altitude mixing programs such as the LAPP. The third modification requires the use of a more sophisticated aft-plume program, which was not available for this study. In lieu of sophisticated plume programs capable of computing variable pressure effects, some simple adjustments to parallel-flow models can be made. The pressure behind the trailing shock is several times higher than the pressure in the base region. The plume core pressure is less than the nozzle exit pressure and may be reduced considerably below ambient because of expansion toward the low-pressure base region. The minimum core pressure may be approximated by calculating the expansion from the throat radius r_t to the slipline radius r_s using the standard equations for isentropic expanding supersonic flow. This leads to sharp pressure discontinuities across the trailing shock and lip shock. Although these discontinuities can be dealt with by piecemeal solution of the problems, only an aft-plume model capable of handling radial pressure discontinuities can solve the problem adequately. If the pressure gradient effects are ignored, serious errors may occur in the plume core mass flow and temperature calculations which will affect the entire aft-plume.

In order to combine the base region with the LAPP, the following steps have been followed:

- 1) Run the BYU base code to obtain base pressure, base equilibrium species concentrations, radial concentration contours, velocity fields in regions 1-6 of Fig. 2, trailing shock pressure and location, slipline starting location, and direction.
- 2) Run an equilibrium combustion code^{16,17} substituting Eqs. (4) and (5) for Eq. (6) to determine temperatures and concentration values in slipline shear layers.
- 3) Determine concentration, velocity, and temperature contours for input to the LAPP code.
- 4) Run the starting line (first longitudinal point) of the LAPP code to be certain that the starting conditions are as desired. Adjust as necessary.

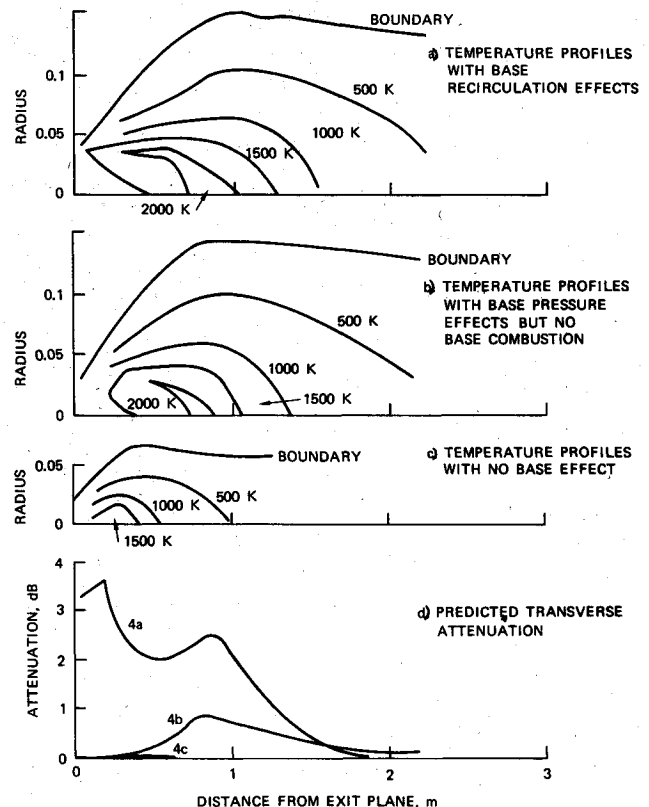


Fig. 4 Results of plume calculations on double-base propellant (Mach 1.67 freestream, 450-m alt, 3-cm nozzle exit diameter, 12.7-cm base diameter, chamber pressure = 6.7×10^6 Pa, $\epsilon = 4.3$).

5) Run the LAPP code to the plume length desired.

Results of this procedure are given for several cases in the next section. The slipline itself is ignored in the input to the LAPP code (step 3 of the foregoing). Because the LAPP code can handle only a limited number of radial input points, the slipline shear layer must be input at only one or at most two radial points. This means that an effective temperature, velocity, and species set must be determined for this region.

Figure 3 shows schematically the coupling of the base and constant-pressure aft-plume codes. The selection of the starting stream-tube grid points also is shown (in this case with only one point, number 12, in the starting slipline shear layer).

It should be noted that in no case were we able to deal with radial pressure gradients, nor did we attempt any manipulation of plume pressures to simulate such gradients. In several runs we did adjust longitudinal pressure by Eq. (3), but this had little effect on the results and increased the run time and computer charges.

Sample Calculations

Temperature profiles from calculations on a double-base propellant are shown in Fig. 4. The calculation made with base recirculation is shown in Fig. 4a; Fig. 4b shows essentially the same size plume without base effluent. Both of these plumes are overexpanded because of the pressure drop in the base region. The much smaller plume of Fig. 4c results from totally ignoring the base region and simply allowing the plume to expand to ambient conditions. The importance of base recirculation on nonequilibrium electron chemistry is shown in Fig. 4d, where predicted transverse X-band attenuation is a clear indication of the elevated electron density emerging from the base region.

The differences between Figs. 4b and 4c are indicative of the size uncertainty that the pressure gradients in the plume can cause. We should expect the initial large plume diameter to shock down to the smaller size in a few shock wavelengths

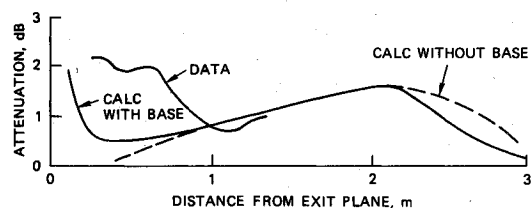


Fig. 5 Transverse K-band attenuation, effect of base on plume of a composite propellant (Mach 2 freestream, 8.2-km alt, 6.1-cm nozzle exit diameter, 32-cm missile base diameter, chamber pressure = 8.6×10^6 Pa, $\epsilon = 9$).

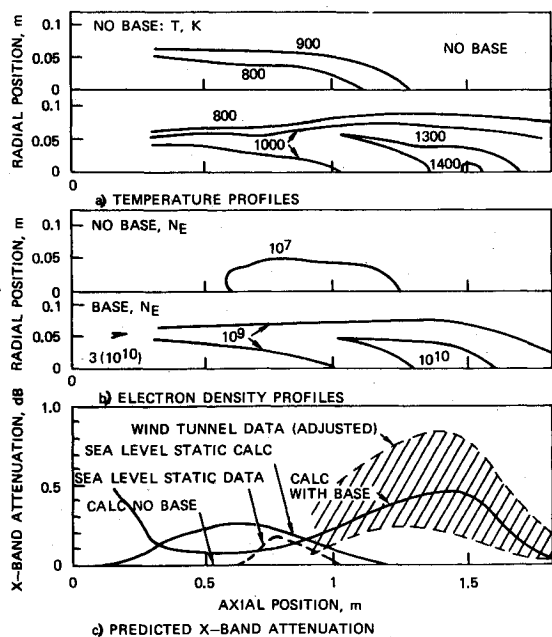


Fig. 6 Comparison of calculated plume properties for propellant C. Effect of base on aft-plume (Mach 2.2 freestream, 7.6-km alt, 4.2-cm nozzle exit diameter, 12.7-cm base diameter, chamber pressure = 4×10^6 Pa, $\epsilon = 4.3$).

(5 to 10 exit diameters). More work must be done on this area of uncertainty. Although there are no wind-tunnel or flight data for this propellant with which to compare the calculation, it is interesting to note that flameholders must be placed in the exhaust in order to stimulate and stabilize afterburning at sea-level static test conditions.¹⁸

In Fig. 5, the results of K-band attenuation calculations for a composite propellant (12% Al, 76% ammonium perchlorate) are shown. This exhaust is sufficiently hot at the exit to burn without the increased temperature and radical species concentrations induced by the base. Hence, the only significant effect of the base is a higher value of attenuation (and O, H, OH, and e^- concentrations) near the nozzle exit. Wind-tunnel data are included in the figure¹ only to show comparability. It is believed that the peak in the data is due to the first strong normal shock (and not to base burning, which was visible only in the test during tailoff), an effect completely ignored in the calculations.

One of the most interesting situations is relayed by Fig. 6, which shows the results of calculations on a nonmetalized propellant containing 24% polyurethane and 75% ammonium perchlorate. Attenuation measurements on this propellant have been published¹ (propellant C) including static sea-level, wind-tunnel, and flight data. In the wind-tunnel tests, the results were very sensitive to freestream Mach number. Below Mach 2.8, afterburning did not appear, and attenuation was so low as to be unmeasurable. At Mach 2.8 and above, base burning induced aft-plume combustion and attenuation rose to levels comparable with those in Fig. 6. Figure 6a shows

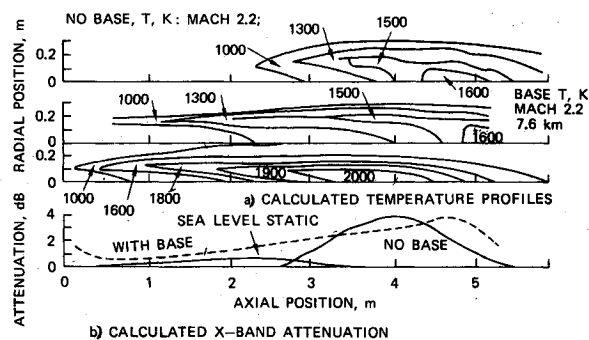


Fig. 7 Calculated full-scale plume properties for propellant C (Mach 2.2 freestream, 7.6-km alt, 13.4-cm nozzle exit diameter, 40.6-cm base diameter, chamber pressure = 4×10^6 Pa, $\epsilon = 4.3$).

temperature calculations for this propellant at 7.6-km alt, Mach 2.2, with a 12.7-cm-diam missile base and 4.2-cm nozzle exit diameter ($\epsilon = 4.3$, $P_c = 4 \times 10^6$ Pa). This Mach number was chosen because it corresponds to the onset of vigorous afterburning in flight tests of this propellant in a motor the size of that analyzed in Fig. 7. It is obvious that the calculations without a base effect show no afterburning at all, whereas the effect of the base is to cause significant afterburning and, as is shown in Fig. 6b, a drastic increase in electron density. A sea-level attenuation prediction and wind-tunnel data are shown, along with predicted attenuation for simulated flight conditions, in Fig. 6c. The wind-tunnel data were obtained with a motor of about four times lower thrust than that for which the calculations were made. The base diameter was the same for both cases. The wind-tunnel data in Fig. 6c have been adjusted by doubling the value on the abscissa. This adjustment should compensate partially for the difference between thrust in the measured and calculated cases.

When the plume size is scaled up to that actually tested in flight (40.6-cm base diameter, 13.4-cm nozzle exit diameter), the base effect is calculated no longer to be critical to the initiation of in-flight afterburning or attenuation, although the base effect causes afterburning to start much closer to the nozzle exit. The same base-diameter-to-nozzle-exit-diameter ratio is maintained in Figs. 6 and 7. The results shown in Fig. 7 are compatible with diagonal microwave attenuation levels up to 20 dB, which were measured in flight tests of propellant C. The in-flight data have been reproduced fairly well by combining the results shown in Fig. 7 with electromagnetic propagation calculations, which include refraction and diffraction effects.

Conclusions

From the calculations performed for this paper, we speculate that the major effect of combustion in the base region is to increase the level of free radicals and charged species that flow into the rest of the plume. Another important effect may be the formation of a stronger first normal shock (due to increased expansion of the core flow). Increased mixing and a somewhat hotter boundary layer near the nozzle also occur. These combined effects will tend to cause afterburning of fuel-rich exhausts, even those that leave the nozzle at low temperatures (below 1000 K). For hot fuel-rich exhausts, which afterburn without flameholder action, the calculated effect of the base on the plume is negligible except in the immediate vicinity of the base itself (see Fig. 5).

It has been observed in flight tests¹ that some plumes afterburn only at speeds above a certain minimum value (about Mach 2.2). This off-on effect is not predicted by the model discussed in this paper, but we may speculate that the effect is due to the base region not following the equilibrium assumption of this model, since, in cases with no plume afterburning, no base burning is visible either.

The sample calculations performed for this study also have demonstrated the importance of plume size to afterburning. For example, the case demonstrated by Figs. 6 and 7 with no base effect shows that the larger plume provides sufficient residence time for free radical concentrations to grow to levels necessary for ignition, whereas the smaller plume does not.

The dependence of calculations of the type performed in this study on accurate reaction rate data requires that the uncertainties in these data be reduced by continued research. Even in the short time since these calculations were made, reports of some different rate constants have been received.¹⁹⁻²¹

More analytical work remains to be done on this problem. The obvious next step is to couple the base calculation to a plume model that accounts for shock-induced pressure discontinuities. The effects of chemical kinetics and the actual flow patterns in the base recirculation zone also must be included if the calculation is to predict the onset of combustion in the recirculating zone itself.¹⁰

Acknowledgment

This paper presents results of one phase of the Naval Sea Systems Command "Low Signature Surface Launched Solid Rocket Motor Program," UF31-332-308, coordinated by the Naval Ordnance Station, Indian Head, Md., G.A. Buckle, Program Manager. The author wishes to acknowledge the help of James Mantz of the Naval Weapons Center who operated the Univac 1110 computer and made the necessary computer program modifications.

References

- ¹Victor, A.C., "Plume Signal Interference, Part 1. Radar Attenuation," Naval Weapons Center, China Lake, Calif., NWC TP 5319, Pt. 1, June 1975.
- ²Mikatarian, R.R., Kan, C.J., and Pergament, H.S., "A Fast Computer Program for Non-Equilibrium Plume Predictions," Air Force Rocket Propulsion Lab., Edwards, Calif., AFRPL-TR-72-94, Aug. 1972.
- ³Jensen, D.E. and Wilson, A.S., "Prediction of Rocket Exhaust Flame Properties," *Combustion and Flame*, Vol. 25, Aug. 1975, pp. 43-55.
- ⁴Jensen, D.E. and Webb, B.C., "Afterburning Predictions for Metal-Modified Propellant Motor Exhausts," *AIAA Journal*, Vol. 14, July 1976, pp. 947-953.
- ⁵Harsha, P.T., "Free Turbulent Mixing: A Critical Evaluation of Theory and Experiment," Arnold Engineering Development Center, Arnold Air Force Station, Tullahoma, Tenn., AEDC-TR-71-36, Feb. 1971.
- ⁶Vaglio-Laurin, R., Dash, S., and Boccio, J.L., "A Comparison of Predicted and Measured Infrared Signatures for Plumes of a Small Hydrocarbon Fueled Rocket," General Applied Science Labs., Westbury, N.Y., GASL TM 195, Oct. 1976.
- ⁷Wilson, K.H. and Mikatarian, R.R., private communications, July 1976.
- ⁸Thomas, P.D. and Wilson, K.H., "Efficient Computation of 'Stiff' Chemically Reacting Flow in Turbulent Free Jets," *AIAA Journal*, Vol. 14, May 1976, pp. 629-636.
- ⁹Gosman, A.D., Pun, W.M., Runshal, A.K., Spalding, D.B., and Wolfshtain, M., *Heat and Mass Transfer in Recirculating Flows*, Academic Press, London, 1969.
- ¹⁰Jensen, D.E., Spalding, D.B., Tatchell, D.G., and Wilson, A.S., "Analysis of Recirculating Rocket Exhaust Flows," private communication.
- ¹¹Smoot, L.D., Simonsen, J.M., and Williams, G.A., "Development and Evaluation of an Improved Aft-Plume Model," Naval Weapons Center, China Lake, Calif., NWC TP 5521, Nov. 1973.
- ¹²Beheim, M.A., Klann, J.L., and Yeager, R.A., "Jet Effects on Annular Base Pressure and Temperature in a Supersonic Stream," NASA TR R-125, 1962.
- ¹³Beheim, M.A., "Flow in the Base Region of Axisymmetric and Two-Dimensional Configuration," NASA TR R-77, 1961.
- ¹⁴Pergament, H.S., private communication, April 1975.
- ¹⁵Levenspiel, O., *Chemical Reaction Engineering*, Wiley, New York, 1962, Chap. 5.
- ¹⁶Cruise, D.R., "Notes on the Rapid Computation of Chemical Equilibria," *Journal of Physical Chemistry*, Vol. 68, Dec. 1964, pp. 3797-3802.
- ¹⁷Zelevnik, F.J. and Gordon, P., "Calculation of Theoretical Rocket Performance at Assigned Area Ratios," NASA TN D-1737, 1963.
- ¹⁸McHale, E.T., "Chemical Interpretation of Suppression of Missile Plume Afterburning by Chemical Agents," *JANNAF 9th Plume Technology Meeting*, CPIA Publ. 277, April 1976.
- ¹⁹Kurzus, S.C., "Revised Ionization Kinetics," Lockheed Missiles and Space Co., Huntsville, Ala., LMSC-HREC TR 5-11027, Appendix A, Dec. 1975.
- ²⁰Cohen, N. and Bott, J.F., "A Review of Rate Coefficients in the H₂-Cl₂ Chemical Laser System," The Aerospace Corp., El Segundo, Calif., SAMSO-TR-75-82, March 1975.
- ²¹Jensen, D.E. and Jones, G.A., "Reaction Rate Coefficients for Flame Calculations," PERME, Westcott, England, PERME Tech. Report No. 35, May 1977.